

MCMC Inference for a Model with Sampling Bias: An Illustration using SAGE data.

November 24, 2021

Russell Zaretzki

Department of Statistics, Operations, and Management Science

The University of Tennessee

331 Stokely Management Center, Knoxville, TN, 37996

email: rzaretzk@utk.edu

and

Michael A. Gilchrist

Department of Ecology and Evolutionary Biology,

The University of Tennessee

569 Dabney Hall, Knoxville, TN, 37996

email: mikeg@utk.edu

and

William M. Briggs

Dept. of Mathematics

Central Michigan University

email: mattstat@gmail.com

and

Artin Armagan

Department of Statistics, Operations, and Management Science

The University of Tennessee

405B Aconda Court, Knoxville, TN, 37996

email: aarmagan@utk.edu

Abstract

This paper explores Bayesian inference for a biased sampling model in situations where the population of interest cannot be sampled directly, but rather through an indirect and inherently biased method. Observations are viewed as being the result of a multinomial sampling process from a tagged population which is, in turn, a biased sample from the original population of interest. This paper presents several Gibbs Sampling techniques to estimate the joint posterior distribution of the original population based on the observed counts of the tagged population. These algorithms efficiently sample from the joint posterior distribution of a very large multinomial parameter vector. Samples from this method can be used to generate both joint and marginal posterior inferences. We also present an iterative optimization procedure based upon the conditional distributions of the Gibbs Sampler which directly computes the mode of the posterior distribution. To illustrate our approach, we apply it to a tagged population of messenger RNAs (mRNA) generated using a common high-throughput technique, Serial Analysis of Gene Expression (SAGE). Inferences for the mRNA expression levels in the yeast *Saccharomyces cerevisiae* are reported.

KEYWORDS: Statistical Analysis of Gene Expression(SAGE), Gibbs Sampling, Biased Sampling.

1 Introduction

This paper develops methods for making Bayesian inferences about the composition of a population whose members have different probabilities of being observed. Our approach applies to situations where the categorical composition of a population is of interest and where some members of the population may be more easily observed than others. The sampling process can be viewed as a multinomial process where the probability of a sample being chosen will differ for each category in a known way. An example: survey samples of males and female birds that differ greatly in their coloration, markings, and degree of vocalization. Alternatively, sampling rates may be differentiated by age classes or species that differ in their activity level or size. Similar problems exist in studies of molecular biology where observations are generally indirect and the ability to observe a molecule varies by type. Specific examples include proteins that differ in their hydrophobicity or size. We will illustrate our ideas, by considering a data set generated using Serial Analysis of Gene Expression (SAGE), a bioinformatic technique used to measure mRNA expression levels.

SAGE is a high-throughput method for inferring mRNA expression levels from an experimentally generated set of sequence tags. A SAGE dataset consists of a list of counts for the number of tags that can be unambiguously attributed to the mRNA of a specific gene. These observed tag counts can be thought of as a sample from a much larger pool of mRNA tags. The tag counts are then used to make inferences about the proportion of mRNA from each gene within the mRNA population from a group of cells. The standard approach for interpreting SAGE data is through the use of a multinomial sampling model (Velculescu et al., 1995, 1997). Morris et al. (2003) directly applied a Bayesian multinomial-Dirichlet model to the observed vector of tag counts. This approach improves upon most earlier work by considering simultaneous inference on all proportions. They provide a simple computationally tractable approach and consider the result of the statistical shrinkage effect

which offers improved estimates for proportions with low tag counts while underestimating the expression proportions for tags with large counts. This leads them to propose a mixture Dirichlet prior in order to mitigate the propensity to underestimate highly expressed genes.

An alternative analysis, which was not based on a multinomial model directly, was developed by Thygesen & Zwinderman (2006), who modeled the marginal distribution of the counts across tag types as though they were independent observations from a Poisson distribution. They applied a hierarchical zero-truncated Poisson model with mean parameter which followed either a gamma or log-normal distribution. A non-parametric adjustment factor was required in order to correctly capture the overabundance of larger counts. Similar analysis (Kuznetsov et al., 2002; Kuznetsov, 2006) modeled SAGE counts using a discrete Pareto-like distribution. These studies found that this model effectively predicted counts greater than zero. One drawback is that the variance of expression cannot be explicitly separated from sample variance. However, in the context of differential expression, Baggerly et al. (2003) suggests that treating genes individually offers less power than a model, such as the multinomial, which incorporates all tags simultaneously.

One common thread is the explicit assumption that an mRNA's frequency in the sampled tag pool is equivalent to its frequency in the mRNA population from which the tag pool was derived. However, because the ability to form tags from an mRNA transcript varies from gene to gene, the tag pool that is sampled is actually a biased sample of the mRNA population (Gilchrist et al., 2007). Gilchrist et al. (2007) illustrated how the tag formation bias could be estimated and incorporated through the calculation of a gene specific tag formation probability. The complicating factor is that the sampling bias of one gene is not only a function of its own tag formation probability, but is also inversely proportional to a mean tag formation probability where the contribution of each gene to this mean is weighted by its frequency in the mRNA population, i.e. the very parameters we wish to estimate.

As a result of the sampling bias, the probability of observing an individual gene depends

on both its tag formation probability and the distribution of these probabilities across all other genes weighted by their mRNA frequency. Gilchrist et al. (2007) derive an implicit solution for the maximum likelihood and joint posterior mode estimators of the composition of the mRNA population. However, there are a number of numerical stability issues that severely limit the range of prior parameters that can be used, i.e. those priors with appreciable weight relative to the observed sample sizes. There is also the restrictive assumption that the contribution of an individual gene to the weighted average is small in order to derive approximations for the marginal credible sets for a given gene. We introduce several new hierarchical models for the posterior distribution of the mRNA proportions given the bias in the observed data. These methods are more robust, flexible, and require fewer assumptions than the analytic approach outlined in Gilchrist et al. (2007).

In addition to the bias introduced through the tag formation process itself, other steps in the experimental process can introduce errors which will affect the ability to interpret SAGE data. These include sampling error, sequencing error, non-uniqueness and non-randomness of tag sequences (Stollberg et al., 2000). For example, the use of PCR to amplify mRNA samples can introduce copying errors into tag sequences. Tags are identified via DNA sequencing, which is an imperfect processes and errors occur on a per nucleotide basis. As a result the error rate depends on the length of the tag's generated. A number of sophisticated techniques have been developed to correct for such errors (Colinge & Feger, 2001; Akmaev & Wang, 2004; Beissbarth et al., 2004). In this study we ignore such complications but believe that it is also possible to address these sources of error by incorporating them into a more complicated model of the experimental process.

Because we are using SAGE data as an illustration, Section 2 describes the experimental process used to generate a SAGE data set as well as the sources of biases that can result and additional sources of errors. Section 3 discusses the basic sampling and inference. Section 3.1 introduces a model for tag formation, and discusses the variation in tag formation. It

also introduces a posterior distribution which explicitly considers bias in tag formation and its consequences on inferences for expression rates. Section 4 introduces several approaches to simulate and estimate the posterior distribution. These include both MCMC based sampling methods as well as direct optimization of the posterior. Finally, Section 5 discusses implications of this method for analysis of SAGE and compares this methodology to that discussed by Morris et al. (2003). Further applications of this methodology to SAGE along with more general applications of the models are also discussed.

2 The SAGE Methodology

The goal of a SAGE experiment is to sample the mRNA population within a group of cells and was developed by Velculescu et al. (1995). Broadly speaking, the SAGE method generates a set of short sequence-based cDNA tags from the mRNA population of a group of cells. Initially, a pool of mRNA is extracted from a group of cells. The unstable single stranded mRNA is reverse transcribed into a double stranded DNA copy (cDNA) using a modified primer that allows the cDNA to be bound to a streptavidin bead. The cDNA is cut into small ‘tags’, using restriction enzymes, which are concatenated together into longer cDNA molecules referred to as concatemers. These concatemers are then amplified and sequenced. A cleavage motif of the anchoring enzyme allows the start and stop points of tags to be identified in the sequence data. Each time a tag from a specific gene is observed in the sequence data, it contributes a count to the dataset. The data is then summarized by the number of tag counts for each individual gene within a genome, which are then used to make inferences about the mRNA population within a group of cells.

The restriction enzymes used to create the tags only cut at very specific sites within the cDNA. For example, the restriction enzyme used by Velculescu et al. (1995) could only cleave the cDNA at the four nucleotide motif CATG. Thus, tags can only be created at specific

points within a gene. Because the site where the cDNA is cut serves as an ‘anchor’ between tags, the restriction enzyme used is often referred to as the anchoring enzyme (AE). We also refer to the specific points in the cDNA cleaved by the anchoring enzyme as AE sites.

While some genes will have no AE sites, many genes will have multiple sites at which the AE could cleave the cDNA. Given that the AE is expected to act in a site-independent manner, a single cDNA molecule can be cut by the AE in multiple places. However, because only the fragment of cDNA that is attached to a streptavidin bead is retained during the experimental process, the site closest to the bead (i.e. the 3’ most site) that is actually cleaved is the only site that can lead to an observable tag (see Figure 1). If the AE worked with 100% efficiency, then each mRNA could only lead to one observable tag. However, the cutting efficacy of the AE is always less than 100% and as a result multiple tags may be generated due to the multiple copies of a gene’s mRNA in the mRNA population of interest. We discuss the overall probability that a gene’s mRNA transcript can be tagged as well as the expected distribution of the tags it can form in Section 3.1. The critical point is that differences in the number of AE sites between genes result in different probabilities that their mRNA will form a tag. Genes whose mRNA transcript lacks any AE site represent a most extreme example of this bias since such genes have zero probability of forming a tag. Such genes are impossible to observe using the SAGE methodology. A further complication is a lack of independence between the mRNA sequences of different genes. This is mainly due to the fact that most genes are the result of gene duplication events. While most genes do contain an AE site, many of these sites lead to non-unique or ‘ambiguous’ tags which cannot be readily assigned to a particular gene. Ambiguous tags are ‘uninformative’ using current technologies; tag-to-gene mapping is discussed at length in Vencio & Brentani (2006).

Experimentalists have attempted to deal with the problem of ambiguous tags by increasing the size of the tag and, thus, decreasing the probability a tag can be attributed to more than one gene. The actual tag length depends on the specific tagging enzyme used (which is

another type of restriction enzyme), but is invariant within an experiment. Initially SAGE tags were 14 bp long. However, four of these bp reflect the cutting motif of the AE and, as a result, were shared by all tags. Experimental advances have been able to extend the tag length to over 20 bp. For example, ‘SuperSAGE’ techniques can lead to tags up to 26 bp long (Matsumura et al., 2003, 2006). Unfortunately, extending the length of a tag comes at a cost (Stollberg et al., 2000). This is because neither the reverse transcription, the PCR amplification, or sequencing process is error free. For example, Velculescu et al. (1997) estimate that the sequencing error rate of a tag is 0.007/bp, thus the probability of obtaining an error free tag decreases geometrically with sequence length, ranging from approximately 10% to 15% in 14 and 22 bp tags, respectively. Transcription errors, either by the cell or during the conversion to cDNA or amplification by the experimentalist, can create either novel ‘orphan’ tags which cannot be mapped to a particular gene or misleading tags which are attributed to the wrong gene.

3 Basic Statistical Inference

Before the SAGE tag counts are considered, we assume that the data is processed to retain only informative tags, i.e. all ambiguous or orphan tags are removed, as is standard practice. The result can be viewed as a vector of observed tag counts for individual genes, i.e. $\mathbf{T} = (t_1, \dots, t_k)$ where k is the number of genes that contain at least one unambiguous AE site and t_i is the sum of all counts which can be uniquely attributed to gene i . It is natural here to view this vector as a sample from a multinomial distribution with k categories. Thus $\mathbf{T} \sim \text{Multi}(T_{tot}, \boldsymbol{\theta})$ where θ_i represents the frequency of gene i tags in the tag pool and T_{tot} represents the total number of informative tags sequenced, i.e. $T_{tot} = \sum_j t_j$. Until recently, inferences about a gene’s frequency in the mRNA population, the population of interest, were assumed to be equivalent to any inferences made about its tag frequency, i.e. the tag pool

was viewed as an unbiased sample of the mRNA population. As pointed out by Gilchrist et al. (2007), this equivalence only holds when all genes have the same tag formation probability. Given the variation between genes, this condition will never be met. Consequently, genes with greater than average tag formation probabilities will be over-represented in the tag pool. Conversely, tags with a lower than average tag formation probability will be under-represented. This sampling bias in the formation of the tag pool, however, can be estimated and used to correct the inferences made from the SAGE data. The first step in adjusting for this bias is the calculation of the tag formation probabilities for every gene in the genome.

3.1 Biased Sampling and Tag Formation Probabilities

As pointed out in Section 2, only cDNA that is attached to a streptavidin bead is retained during the experimental process. As a result, tags are created from the 3' most AE site that is actually cleaved (Figure 1). Let k_i be the number of restriction enzyme sites which may be cleaved by the AE on mRNA generated from gene i , let p be the probability the AE will cleave a site, and assume that cleavage probability is independent between sites and does not vary between genes. If we label sites 1 through k_i starting at the 3' most site (i.e. the site closest to the bead; see Figure 1). It follows that the probability of generating a tag through AE cleavage at site $j \in \{1, \dots, k_i\}$ is $(1 - p_i)^{j-1} p_i$. This corresponds to the probability of no cleaving in sites 1 to $j - 1$, and a cleaving at site j . Note that this probability is independent of what happens at the AE sites 5' from the j th site. Thus, the probability of creating a tag at site j on an mRNA generated from gene i follows a geometric distribution. The fact that the expected distribution of tags varies with AE cleavage probability p can be used to estimate p from the set of intra-genic tag distributions (Gilchrist et al., 2007).

If the set of tags which can be created from the AE sites within a gene's mRNA transcript are all informative (i.e. can be uniquely assigned to a single gene), the probability of gener-

ating any of the possible tags from the i th category of mRNA is

$$\phi_i = \sum_{j=1}^{k_i} (1-p)^{j-1} p = 1 - (1-p)^{k_i}. \quad (1)$$

When ambiguous tagging sites occur within a gene’s mRNA transcript, say sites l and m , these sites are simply excluded from the summation over j in eq. (1). The reduction in ϕ_i due to tag ambiguity is greatest when an ambiguous tag is formed at the 3’ most AE site (site 1 in Figure 1) and is least when such a tag occurs in the 5’ most AE site (site k_i). But note that it is possible for transcripts to have multiple ambiguous AE tag formation sites. For purposes of our analysis, we will assume that the value of ϕ_i has been estimated for all genes and treat these as *known* constants (see Gilchrist et al. (2007) for a more details on these calculations). The variation in the tag formation probability between genes stems from the two basic facts. First, genes vary in the number of AE sites they contain. Second, genes also vary in the number and location of AE sites which are ambiguous. As a result the tag pool represents a biased sample of the mRNA population of interest. The degree of bias exhibited is a function of both the distribution of tag formation probabilities across the genome, and the distribution of these genes within the mRNA population itself, as we will now demonstrate.

3.2 Maximum Likelihood and the Joint Posterior Distribution

As discussed earlier, an obvious model for the observed tag data is the multinomial distribution. Let $T_{tot} = \sum_{i=1}^k t_i$ be the total count of all observed tags. Then

$$P(T|\theta) = \binom{T_{tot}}{t_1, t_2, \dots, t_k} \prod_i \theta_i^{t_i}$$

where θ_i are the frequencies of tags in the tag pool. Section 3.1 indicates that frequency of SAGE tags generated from gene i is,

$$\theta_i = \frac{m_i \phi_i}{\sum_j m_j \phi_j} \quad (2)$$

where, we remind the reader, that ϕ_i is *known* and represents the probability that a mRNA strand from gene i in the group of cells will be converted into a tag and where m_i , the quantity of interest, is the relative proportion of mRNA from gene i in those cells. Hence, the bias corrected likelihood model is,

$$P(T|\mathbf{m}) = \binom{T_{tot}}{t_1, t_2, \dots, t_k} \prod_i \left(\frac{m_i \phi_i}{\sum_j m_j \phi_j} \right)^{t_j} \quad (3)$$

Because the vector $\mathbf{m} = \{m_1, m_2, \dots, m_k\}$ is a vector representing relative proportions, or equivalently the probability that an individual mRNA strand represents gene i , the components of \mathbf{m} must satisfy the conditions: $m_i \geq 0$ and $\sum_{i=1}^k m_i = 1$.

Direct maximization of the likelihood with respect to the parameters m_i is straightforward via the invariance property of the MLE. Consider the observed sample proportion $\hat{\theta}_i = t_i/T_{tot}$. Given constraints on the possible values of m_i and equation (2), the MLE estimates of $\hat{\mathbf{m}} = \{\hat{m}_1, \hat{m}_2, \dots, \hat{m}_k\}$ must satisfy the following equality,

$$\sum_i^k \frac{\hat{\theta}_i}{\phi_i} = \frac{1}{\sum_i^k \hat{m}_i \phi_i}. \quad (4)$$

While estimation of the MLE is relatively straightforward, estimating confidence intervals for \mathbf{m} is difficult. The existence of the normalization term $\sum_j m_j \phi_j$ in the denominator of the l.h.s. of eq. (4) makes computation of the information matrix taxing, particularly for the large dimensional vectors encountered when working with SAGE data (i.e. k is of the order 10^3 to 10^4). In addition, because the number of categories is generally within an order

of magnitude of, or possibly even greater than, the number of tags sampled, most categories have either zero or only a few observations. These relatively small cell counts make any inferences based on asymptotic approximations questionable.

As an alternative, we consider a Bayesian approach to the problem. The constraints lead naturally to the assumption of a Dirichlet prior on \mathbf{m} ,

$$\mathbf{m} \sim D_k(\alpha_1, \dots, \alpha_k) = \frac{\Gamma(\sum \alpha_i)}{\prod_{i=1}^k \Gamma(\alpha_i)} \prod_{i=1}^k m_i^{\alpha_i-1}.$$

Combining this prior distribution with the likelihood function Equation 3 leads to a posterior distribution proportional to the product

$$[\mathbf{m}|\mathbf{T}] \propto \left(\sum_{i=1}^k m_i \phi_i \right)^{T_t} \prod_{i=1}^k (m_i \phi_i)^{\alpha_i + t_i - 1} \quad (5)$$

Gilchrist et al. (2007) discuss methods for the direct maximization of this quantity and also discuss the choice of a prior and its consequences on the marginal inferences of m_i for particular values of i . A main inferential difficulty is the existence of the normalizing term $\sum_{i=1}^k m_i \phi_i$ which is required to force the values θ_i to sum to one. Because the form of the posterior is not standard, this leads to difficulties when trying to numerically estimate the normalizing constant. Therefore, we adopt a Monte-Carlo approach to inference on the posterior distribution.

4 Gibbs Sampling Strategies for Posterior Analysis

We explicitly consider three strategies to simulate from the posterior distribution given by eq. (5). The first strategy is presented in Subsection 4.1. This approach extends the Binomial - Poisson hierarchical model of Cassella and George given in Arnold (1993). Given a random count T_i , this model proposes a binomial distribution $T_i \sim \text{Binomial}(g_i, \phi_i)$. g_i ,

the number of trials, is assumed to be Poisson distributed and represents the total number of mRNA's of a given type in the cells. Here, we extend the model to take into account the multinomial nature of the original mRNA population. The second strategy is presented in Subsection 4.2. This approach proposes that a count $T_i \sim \text{Binomial}(g_i, p)$ and that the vector $\mathbf{g} \sim \text{Multinomial}(N, \mathbf{m})$. We believe this strategy represents the data generating process of SAGE slightly more realistically than the first strategy. Finally, in Subsection 4.3 we consider a missing data strategy. This approach applies a modified version of the conjugate Dirichlet-Multinomial model and is more computationally expedient than the first two strategies. Overall, each of the three strategies offers its own unique strengths and weaknesses, which we discuss below.

The algorithms discussed were all applied to a published SAGE data set which analyzed the yeast *Saccharomyces cerevisiae* (Velculescu et al., 1997). In particular, data collected from the log-phase were analyzed. There were 6096 genes included in the data. The maximum tag count was 392 and the minimum was zero. 3560 of the genes included had observed counts of 0. Gene dependent sampling probabilities ranges from $\approx .003$ to 1. Tag assignments to unique genes and assignment of non-unique tags for this analysis were described in Gilchrist et al. (2007). All simulations described below were computed using R (Version 2.3.1) on dual core Intel desktop computer running Linux Fedora 5.

In what follows, the symbol \mathbf{T} will represent the vector of observed tag counts, ϕ the known vector of gene dependent sampling probabilities, \mathbf{g} a latent vector representing the actual number of mRNA's from each gene, \mathbf{m} the vector of mRNA proportions and N the total mRNA copy number in the cell. Throughout this analysis, we assume that gene dependent tag formation probabilities ϕ_i are known constants.

4.1 Gibbs Sampling based on a Dirichlet-Poisson-Binomial Model.

Mechanically, the SAGE technique proceeds as discussed in Section 2 where the pool of mRNA from the cells are first converted to cDNA, tagged and then amplified. In the model discussed below, inspired by Cassella and George, we assume that a fixed population of mRNA's exists of size N which we will suppose is random within the cells. The total size N is determined by a gamma distribution which is rounded off to the nearest integer. The choice of gamma here is convenient due to its role as a conjugate prior. Given the population of size N , the relative proportions m_i of different categories of mRNA are unknown and may be modeled as a Dirichlet distribution with prior $\alpha = (\alpha_1, \dots, \alpha_k)$ where the α_i will often be chosen to be identical, i.e. $\alpha_i = c \forall i$ and some constant c .

Because cells contain mRNA transcripts from thousands of different genes, the probability of seeing any particular gene is low. It is therefore logical to assume, given N and m_i , that the actual number of mRNA's of a certain type $g_i, i = 1, \dots, k$, extracted from the group of cells, satisfies a Poisson law with mean $\mu = N \cdot m_i$. Finally, the restriction enzyme process generates a tag count t_i for a particular complimentary DNA strand in a binomial fashion based upon the tag formation probability ϕ_i . Hence, the hierarchical data generating mechanism follows, $T_i \sim Binomial(g_i, \phi_i)$, $g_i \sim Poisson(N * m_i)$, $\mathbf{m} \sim Dirichlet(\alpha_1, \dots, \alpha_k)$, $N \sim ceiling(Gamma(\gamma_1, \gamma_2))$. We refer to this model as the Dirichlet-Poisson-Binomial (DPB) model. A first weakness of this model is that the sum of all counts $\sum g_i$ may not add up to the total counts N . However, this approach allows us to infer the total population size N . In constructing this hierarchical model, we have essentially provided a multivariate extension of the model investigated in Thygesen & Zwinderman (2006) while integrating the

sampling bias. Together, the elements described above give a joint posterior distribution,

$$[\mathbf{m}, \mathbf{g}, N | \mathbf{T}, \boldsymbol{\alpha}, \gamma_1, \gamma_2] \propto \prod_{i=1}^k \binom{g_i}{t_i} \phi_i^{t_i} (1 - \phi_i)^{g_i - t_i} \frac{e^{-Nm_i} (Nm_i)^{g_i}}{g_i!} \\ \times m_i^{\alpha_i - 1} e^{-\gamma_2 N} N^{\gamma_1 - 1}$$

From this expression, we can deduce the set of full conditional distributions (Ghosh et al., 2006),

$$[m_i | t_i, g_i, N, \boldsymbol{\alpha}, \gamma_1, \gamma_2] \sim \Gamma(g_i + \alpha_i, N) \\ [g_i | \mathbf{T}, \mathbf{m}, N, \boldsymbol{\alpha}, \gamma_1, \gamma_2] \sim t_i + \text{Poisson}(Nm_i(1 - \phi_i)) \\ [N | \mathbf{T}, \mathbf{g}, \mathbf{m}, \boldsymbol{\alpha}, \gamma_1, \gamma_2] \sim \Gamma\left(\sum_{i=1}^k g_i + \gamma_1, 1 + \gamma_2\right)$$

A Gibbs sampler can be implemented based on this full set of conditionals; however, a second weakness of this approach is the need to update each value of m_i independently. Because the vector \mathbf{m} is typically on the order of thousands or tens of thousands, this is a costly computation.

In order to minimize autocorrelation between samples, our experiments stored only the last of every hundred samples for analysis. Inference for means was based upon the final 1000 of these stored samples drawn after an extensive burn in period of 400,000 simulations. The two prior parameter vectors tested were $\boldsymbol{\alpha} = 1$ and $\alpha_i = 1/k \forall i$. $k = 6096$ is the number of genes in the sample. The distribution of population size, N , used a shape parameter $\gamma_1 = 100$ and prior scale $1/\gamma_2 = 200$. The mean of a gamma with these parameters is 20000 which is somewhat larger than a natural estimate of the population size, $\sum_i (t_i/\phi_i) = 16438.81$. This was chosen intentionally to determine if the posterior would converge to a reasonable estimate of N . Experimentalists assume that there are $\sim 15,000$ mRNA in a cell which also

justifies this assumption.

As mentioned above, in addition to lags of 100 between samples, a very large burn-in period was used in the analyses of Sections 4.1 – 4.3. In order to ensure that autocorrelation did not adversely effect parameter estimates, some basic convergence analysis was performed. Convergence was evaluated on 2 sampled quantities, the total mRNA population size N and the gene at the third locus in the data set: YAL003W. Both quantities have direct inferential value and autocorrelation could adversely affect estimates. YAL003W was selected randomly among the set of genes with medium to large tag counts. Out of the 12799 tags observed, 32 could be attributed to gene YAL003W. Direct autocorrelations of both sequences were tested at various lags. Table 1 examines correlations among samples for different lags and suggests that for inference on proportions m_i , autocorrelations are very low between samples with lags as small as 10. Conversely, correlations, for sample size N are extremely high leading to much less reliable inference.

In practice, if only the vector \mathbf{m} is of interest, far fewer samples are needed which would significantly speed up the algorithm. Physical timings for runs of these and other algorithms are given in Table 2. These show that as executed, this algorithm required about 11-12 hours to run. If only every 10th sample were collected, 50,000 total samples, the algorithm would have required approximately 1 hour.

In order to understand the behavior of the proportions, we compared various estimates of the m_i . These include posterior means from the Gibbs sampler, standard MLE's, corrected MLE's based on Formula 4, and analytically derived posterior modes from Gilchrist et al. (2007). In addition, 95% posterior credible regions are also computed. Figure 2 plots the above quantities versus rank for the 20 genes with largest tag counts. Rank 1 corresponds to the most frequent gene and the prior used is $\alpha = 1$. As one would expect, the corrected MLE and the posterior mode coincide perfectly in this case. Both posterior means and posterior modes based on the biased sampling correction deviate strongly from the standard

MLE for many of the most frequently tagged genes. Posterior modes and means follow nearly identical trends with the modal estimates being uniformly larger. As one can see, modal estimates typically lie slightly above the 97.5th percentile of the simulated posterior distribution in this case.

Figure 3 summarizes results when each $\alpha_i = 1/k$. This parametrization corresponds to a U-shaped prior distribution. Here one can see the i^{th} corrected MLE and posterior mean now coincide almost perfectly while the posterior mode lies at or above the 97.5th percentile of posterior samples. Again, all estimators deviate significantly from the unadjusted MLE's. Due to the similarity of the corrected MLE and posterior mean, it is tempting to interpret the posterior intervals as frequentist confidence intervals. To date, no work has been done to verify the frequentist coverage properties of these intervals.

For inferential purposes, the posterior mean vector and both joint and marginal intervals can be derived from the Monte Carlo samples. However, as discussed below in Section 5, it may be useful to compute the joint posterior mode for use as an estimator. For example, the posterior mode reduces to the MLE when the parameter $\alpha_i = 1$ for all i . A second advantage of this model is that the joint mean can be computed through the Lindley-Smith maximization method (Lindley, D. V. & Smith, A. F. M., 1972; Chen et al., 2000).

Lindley and Smith proved that an algorithm that iteratively maximized each of the full conditional distributions will eventually converge to the global maximum of the posterior. Because each of the conditionals in this model has a closed form expression for its maximum, this optimization approach is both simple and extremely fast. Similar to Gibbs sampling, this procedure starts from an arbitrary point. Maximization proceeds by iterating across the full set of conditional distributions, maximizing each and substituting the maximum into the next conditional. The hierarchical model considered here is not identical to eq. (3), but depends upon hyperparameters (γ_1, γ_2) which effect the mode of the posterior distribution. One possibility for choosing these hyper-parameters is to pick them to minimize the distance

between analytical mode and iteratively computed mode.

Algorithm 1: Dirichlet-Poisson-Binomial posterior mode estimation via the Lindley-Smith algorithm

```

// Initialization
Set the initial values  $\gamma_1, \gamma_2, \mathbf{N}, \mathbf{m}_0, \mathbf{g}$ .
// Main loop

while  $\sum |m_i^{new} - m_i| > 10^{-5}$  do
     $m_i^{new} = \max[\pi(m_i | t_i, g_i, N, \phi, \alpha, \gamma_1, \gamma_2) = (g_i + \alpha) / (N)$ 
     $g_i^{new} = \max[\pi(g_i | \mathbf{T}, \mathbf{m}, N, \phi, \alpha, \gamma_1, \gamma_2) = t_i + \text{floor}(Nm_i(1 - \phi_i))$ 
     $N^{new} = \max[\pi(N | \mathbf{T}, \mathbf{g}, \mathbf{m}, \phi, \alpha, \gamma_1, \gamma_2) = (\sum g_i + \gamma_1) / (1 + \gamma_2)$ 
end

```

4.2 A Dirichlet-Multinomial-Binomial Approach.

A second approach is both more computationally efficient and arguably more directly comparable to the sampling mechanism inherent in SAGE. For convenience, we begin by assuming that the total number of mRNA in the sample is $N \sim Pois(\lambda)$. Given this mRNA population size, the vector \mathbf{g} of counts of each category of mRNA prior to tag formation follows a multinomial distribution,

$$[\mathbf{g} | \alpha] \sim \binom{N}{g_1, g_2, \dots, g_k} m_1^{g_1} m_2^{g_2}, \dots, m_k^{g_k}$$

whose probabilities are the m_i and are assumed to follow a Dirichlet distribution with parameter vector α .

The joint posterior distribution can now be written as,

$$\begin{aligned}
 [\mathbf{m}, \mathbf{g}, N | \mathbf{T}, \alpha, \gamma_1, \gamma_2] &\propto \prod_{i=1}^k \binom{g_i}{t_i} \phi_i^{t_i} (1 - \phi_i)^{g_i - t_i} \frac{e^{-\lambda} \lambda^N}{N!} \\
 &\times \binom{N}{g_1, g_2, \dots, g_k} m_1^{g_1 + \alpha_1 - 1} m_2^{g_2 + \alpha_2 - 1}, \dots, m_k^{g_k + \alpha_k - 1}.
 \end{aligned}$$

Reminding readers that $\boldsymbol{\phi} = (\phi_1, \phi_2, \dots, \phi_k)$ be the vector of known gene dependent tagging probabilities, the full conditional distributions here are,

$$\begin{aligned} [\mathbf{T}|t_i, g_i, N, \gamma_1, \gamma_2] &\sim \text{Dirichlet}(\alpha + G) \\ [\mathbf{g}|\mathbf{T}, \mathbf{m}, N, \boldsymbol{\alpha}, \gamma_1, \gamma_2] &\sim t_i + \text{Multinom}(N - T_t, \mathbf{m} * (1 - \boldsymbol{\phi})) \\ [N|\mathbf{T}, \mathbf{g}, \mathbf{m}, \boldsymbol{\alpha}, \gamma_1, \gamma_2] &\sim \Gamma(T_{tot} + \gamma_2, 1 + \gamma_1) \end{aligned}$$

where $\mathbf{m} * (1 - \boldsymbol{\phi})$ is an element wise product with 1 representing a vector of identical dimension to \mathbf{m} . Hence, the i^{th} element of the vector is given by $m_i(1 - \phi_i)$.

We refer to this hierarchical model as the Dirichlet-Multinomial-Binomial (DMB) model. Inference in this case is much faster because the entire \mathbf{m} vector can be updated at once instead of requiring separate updates for each gene level i . This formulation is also more natural in the sense that it restricts the pre-tagging counts to sum to the population total N . One drawback is that the observed data provides no information for posterior inference about the population size N . A minor drawback of this approach is that it is more difficult to perform a Lindley - Smith maximization to derive the mode. Maximizing the conditional distribution of \mathbf{g} , the vector of mRNA counts, would require maximizing a multinomial distribution over the discrete counts.

Experimental testing of this algorithm provided results similar to the first procedure. Five-million variates were drawn with every hundredth stored. The DMB algorithm was dramatically faster than the DPB approach finishing simulation in just over 30 minutes. Table 1 shows little if any correlation at any lag. For sample size N , this is to be expected since the conditional distributions depend only on the data and hyperparameters which are fixed. We conclude that the algorithm could be accelerated without loss of accuracy by reducing the number of simulations. Inference was based on the final 1000 stored samples. Figure 4 below displays inferential results from this model for the 20 most frequently tagged

genes ranked from largest to smallest. Behavior and trends are almost identical to the DPB model. For the case where all $\alpha_i = 1$, the posterior mean was systematically smaller than the posterior-mode/MLE for cases with large tag counts. The posterior-mode was distinctly different than the unadjusted tag proportions and both sets were above the upper credible bounds for the posterior mean. In the case where all $\alpha_i = 1/k$, the posterior-mean again matches the corrected MLE almost exactly. The posterior mode tracks the mean closely but is always larger and the unadjusted proportions are usually outside the credible region.

4.3 A Missing Data Approach.

Instead of renormalizing the probabilities $\theta_i = (m_i\phi_i)/(\sum m_i\phi_i)$ and doing inference based on the posterior of eq. (5), a second more straightforward approach uses missing data.

Considering again a data generation process as described in section 3.2, we augment the observed data vector T with an extra category which represents any cDNA that is not converted to a SAGE tag. This count is not observed, but if a distribution such as a Poisson is proposed, we may consider a Bayesian approach. The resulting posterior distribution for the data is,

$$[\mathbf{m}|\mathbf{T}, \boldsymbol{\alpha}] \propto (1 - \sum_{i=1}^k m_i\phi_i)^r \prod_{i=1}^k (m_i\phi_i)^{t_i + \alpha_i - 1}$$

where we have assumed a Dirichlet prior on the unknown initial proportions $\mathbf{m} \sim D_k(\alpha_1, \dots, \alpha_k)$. The resulting posterior distribution is a Dirichlet distribution with $k + 1$ categories, compared with the k categories in the initial distribution \mathbf{m} . In particular the distribution is a $D_{k+1}(t_1 + \alpha_1, \dots, t_k + \alpha_k, r + 1)$.

By integrating over the missing data term or otherwise eliminating it, it is possible to sample from the joint distribution whose success probability is $m_i\phi_i$. According to the marginalization property of the Dirichlet (Bilodeau & Brenner, 1999) the distribution of any subset of variables $(\theta_{i_1}, \theta_{i_2}, \dots, \theta_{i_j})$ from a $D_k(\alpha_1, \alpha_2, \dots, \alpha_k)$ with $\sum \alpha_i = p$ is distributed

$D_{j+1}(\alpha_{i_1}, \alpha_{i_2}, \dots, \alpha_{i_j}, q)$. Here $q = p - \sum_{i=1}^j \alpha_{i_j}$ corresponds to the total of the variables being marginalized over. In words, by considering only a subset of j categories we observe a Dirichlet distribution on $j+1$ categories with $\sum_i \alpha_i = p$ remaining the same. In our case, the value of r will be a component of the parameter q . Several modes of inference are available based on this missing data approach. Suppose first that we are particularly interested in the posterior means of the m_i parameters. An exact calculation is possible based upon the marginalization properties of the Dirichlet (Bilodeau & Brenner, 1999, Corollary 3.4).

Theorem 4.1 *Let $\boldsymbol{\theta} = (\theta_1, \dots, \theta_p, \theta_{p+1}) \sim \text{Dirichlet}(\alpha_1, \dots, \alpha_p, \alpha_{p+1})$. Let $\alpha_0 = \sum_{i=1}^{p+1} \alpha_i$. Suppose that $S = \sum_{i=1}^p \theta_i$, and for $j < p$, let $\boldsymbol{\theta}_1 = (\theta_{i_1}, \dots, \theta_{i_j})$ be any subset of components of $\boldsymbol{\theta}$. It follows that $\boldsymbol{\delta}_1 = \boldsymbol{\theta}_1/S \sim \text{Dirichlet}(\alpha_{i_1}, \dots, \alpha_{i_j}, \delta)$ with $\alpha_0 - \alpha_{p+1} = \delta + \sum_{d=1}^j \alpha_{i_d}$*

This result demonstrates that, ignoring the missing categories, the distribution of the

$$\frac{(m_1\phi_1, \dots, m_{k-1}\phi_{k-1}, m_k\phi_k)}{\sum_1^k m_i\phi_i} \sim \text{Dirichlet}(\alpha_1 + t_1, \dots, \alpha_{k-1} + t_{k-1}, \delta),$$

with $\delta = t_k + \alpha_k$. Let $w_i = (\alpha_i + t_i) / \sum(\alpha_i + t_i)$. Then by reweighting, we can compute,

$$E(m_i) = \frac{1}{\phi_i \sum_i w_i} \frac{\alpha_i + t_i}{\sum(\alpha_i + t_i)}.$$

More generally, Gibbs sampling is also available for this problem and extends inference to Bayesian interval estimates. Again observing the posterior distribution,

$$[\mathbf{m}, r | \mathbf{T}, \mu] \propto (1 - \sum_{i=1}^k m_i \phi_i)^r \prod_{i=1}^k (m_i \phi_i)^{t_i + \alpha_i - 1} \frac{e^{-\mu} \mu^r}{r!} \quad (6)$$

The full conditional distributions are derived to be,

$$\begin{aligned}
 [r|\mathbf{T}, \mathbf{m}, \boldsymbol{\alpha}, \boldsymbol{\mu}] &= \text{Poisson}((1 - \sum m_i \phi_i) \mu) \\
 [\mathbf{m}\boldsymbol{\phi}|\mathbf{T}, r, \boldsymbol{\phi}, \boldsymbol{\alpha}, \boldsymbol{\mu}] &= D(r, \alpha_1 + t_1, \dots, \alpha_k + t_k)
 \end{aligned}$$

In order to apply Gibbs Sampler a value for the hyperparameter μ must be selected. In the case where all $\alpha_i = 1$, a logical mean for the Poisson is $T_{tot} \sum_i m_i (1 - \phi_i) / \sum_i m_i \phi_i$ since $\sum m_i (1 - \phi_i) = 1 - \sum m_i \phi_i$ is the probability that an mRNA is not converted into a tag. Equation 4 provides a useful estimate of $\sum m_i \phi_i$.

Like the DPB algorithm above, the missing data algorithm also admits a simple Lindley-Smith optimization procedure in order to compute the posterior mode. If the prior mean of r , $\boldsymbol{\mu} = 10, 100$ then the posterior mode of the missing data model is nearly identical to the exact analytical mode. The mode of the Dirichlet conditional is

$$\widehat{m_i \phi_i} = \frac{t_i + \alpha_i - 1}{\sum_i (\alpha_i + t_i) + r - k}, \tag{7}$$

see Gelman et al. (2005). The mode for the Poisson is the mean rounded down to the nearest smaller integer (Wikipedia, 2007). Results for this case are very similar to the previous two. This algorithm is clearly the fastest, completing 5 million samples in 20 minutes. Autocorrelation in the untagged population size r decreases to 0 after 50 simulations but proportions m_i seem uncorrelated at all lags. Conclusions for Figures 6 and 7 are largely identical to the above. In fact, as implemented quantitative differences do exist between the methods in the case where all $\alpha_i = 1$ with this method providing the smallest or most heavily shrunk estimates of genes with large counts and the DPB method giving the largest estimates. Because probabilities must sum to one, the opposite effect should exist for categories with

small counts although the mass will be spread over thousands of categories leading to very minute differences.

5 Conclusions

Sampling bias is a ubiquitous problem in studying biological problems. This work focuses on a general biasing mechanism of which data generation from in SAGE is a prototype. We present three hierarchical models which provide posterior inference for the biased sampling model given in eq. (3). This work compliments earlier work by Gilchrist et al. (2007) in two notable ways. First, it provides a flexible and efficient methodology which extends the range of the prior distributions that are available. It is important to point out the effect of the typical flat prior $\alpha = 1$ on inference: analogously to the binomial case (Christensen, 1997), this prior assumes that each category was seen once in previous experiments, a very strong assumption due to the small size of the tag sample compared to the number of categories. The result is that the prior overwhelms the data for many of the categories. In the context of SAGE, it may be more appealing to the scientist to choose a weaker prior such as $\alpha = 1/k$, which, as we've seen, gives the actual data more voice. Because the analytical approximations of Gilchrist et al. (2007) do not extend easily to this regime of priors, the simulation based results presented here are increasingly valuable. Second, the more robust methodology presented here provides a foundation for extending the analysis to include more realistic models of the tag formation process (such as the inclusion of transcription or sequencing errors) or more complex priors.

Our approach may be contrasted with Morris et al. (2003), who investigated joint estimators of the relative proportions of different mRNA transcripts in SAGE experiments based on posterior inference from a conjugate Dirichlet-Multinomial model. They note that while the shrinkage properties of the posterior mean provide improved average inference with respect

to squared error loss across all categories, they tend to shrink categories where large counts are observed excessively in order to boost the estimated probabilities of cells with few or no counts. Due to the massive number of categories and the extreme imbalance in observed frequencies (e.g. more than half of the categories have zero counts in our data), the estimates for frequently observed genes tend to be fairly poor. This observation highlights the main weakness of shrinkage estimators, while they perform better on average across categories, they may perform poorly on particular categories which may be of primary interest. Morris et al. (2003) resolve the problem by introducing a hierarchical Dirichlet-Multinomial model which clusters genes into two categories, high and low frequency, partitioning the overall mass in order to mitigate the shrinkage in the high frequency categories.

Our contribution is clearly distinct from that of Morris et al. (2003) since it focuses on a discrepancy in the sampling model. Nevertheless, it should be possible to extend our methods to allow for the mixture priors used by Morris et al. (2003). Even without such an extension, our results offer alternative methods and important insights into shrinkage in models with large or massive numbers of categories. For example, we've shown that by using the prior $\alpha = 1/k$, the posterior mean is equal to the corrected MLE. The additional advantage of a sampling model is that it generates marginal posterior credible sets for the proportion m_i . If inference focuses only on genes with large expression levels, we gain one of the main advantages of Monte Carlo sampling without the concern of excessive shrinkage. If one is only interested in point estimates, and excessive shrinkage is a concern, it may also be appropriate to use the analytical mode as an estimator. For example, the posterior mode for model 5 is identical to the MLE for model 3 when $\alpha = 1$, while the posterior mean becomes equivalent when $\alpha = 1/k$. Given the stated hyper-parameters, posterior means are shrunk for more frequently observed categories and increased for rarely observed categories. The models provide different levels of shrinkage, with the Dirichlet-Poisson-Binomial (DPB) model providing the least, and the missing data model providing the most shrinkage. In

terms of computation time, the DPB method is much less efficient and arguably offers no advantage over the other methods for SAGE. However, in other applications the DPB model may be closer to the model of interest.

A number of important statistical questions remain to be answered. Besides the sampling errors dealt with here, there are other sources of errors inherent in SAGE's tag formation and sampling processes (Stollberg et al., 2000), which future work could address. This analysis also presumed that the category dependent sampling probabilities were fixed when in fact they were estimated from the data. A model that views ϕ as a random quantity would also represent an improvement. Finally, a major emphasis of SAGE analysis regards evaluation of differential expression levels (Baggerly et al., 2003, 2004) between related cell samples. Because the AE cutting probability p is experiment dependent (Gilchrist et al., 2007), it is important that the biasing mechanism be taken into account when evaluating differential expression across experiments. Indeed, this should lead to increased power and accuracy in such studies.

References

- Akmaev, V. R., & Wang, C. J.(2004). Correction of sequence-based artifacts in serial analysis of gene expression. *Bioinformatics*, *20*, 1254-1263.
- Arnold, S. F.(1993). Handbook of statistics. In C. Rao (Ed.), (Vol. 9, p. 599-625). Elsevier Science.
- Baggerly, K. A., Deng, L., Morris, J. S., & Aldaz, C.(2004). Overdispersed logistic regression for SAGE: Modelling multiple groups and covariates. *BMC Bioinformatics*, *5*, 144.
- Baggerly, K. A., Deng, L., Morris, J. S., & Aldaz, C. M.(2003). Differential expression in SAGE: accounting for normal between-library variation. *Bioinformatics*, *19*, 1477-1483.

- Beissbarth, T., Hyde, L., Smyth, G. K., Job, C., Boon, W.-M., Tan, S.-S., et al. (2004). Statistical modeling of sequencing errors in SAGE libraries. *Bioinformatics*, *20 Suppl 1*(NIL), I31-I39.
- Bilodeau, M., & Brenner, D. (1999). *Theory of multivariate statistics*. New York: Springer.
- Chen, M.-H., Shao, Q.-M., & Ibrahim, J. G. (2000). *Monte carlo methods in bayesian computation*.
- Christensen, R. (1997). *Log-linear models and logistic regression* (2 ed.). New York, USA: Springer Verlag.
- Colinge, J., & Feger, G. (2001). Detecting the impact of sequencing errors on SAGE data. *Bioinformatics*, *17*, 840-842.
- Gelman, A., Carlin, B., Stern, H., & Rubin, D. (2005). *Bayesian data analysis* (2 ed.). Chapman and Hall.
- Ghosh, J. K., Delampady, M., & Samanta, T. (2006). *An introduction to bayesian analysis*. New York: Springer.
- Gilchrist, M., Qin, H., & Zaretzki, R. (2007, In Press). *Modeling SAGE tag formation and its effects on data interpretation within a Bayesian framework*. (In Press)
- Kuznetsov, V. A. (2006). Statistical methods in serial analysis of gene expression(SAGE). In W. Zhang & I. Shmulevich (Eds.), *Computational and statistical approaches to genomics* (p. 163-2008). New York: Springer Verlag. (2nd Edition)
- Kuznetsov, V. A., Knott, G. D., & Bonner, R. F. (2002). General Statistics of Stochastic Process of Gene Expression in Eukaryotic Cells. *Genetics*, *161*(3), 1321-1332.

- Lindley, D. V., & Smith, A. F. M. (1972). Bayes estimates for the linear model. *Journal of the Royal Statistical Society. Series B (Methodological)*, 34.
- Matsumura, H., Bin Nasir, K. H., Yoshida, K., Ito, A., Kahl, G., Kruger, D. H., et al. (2006). SuperSAGE array: the direct use of 26-base-pair transcript tags in oligonucleotide arrays. *Nature Methods*, 3, 469-474.
- Matsumura, H., Reich, S., Ito, A., Saitoh, H., Kamoun, S., Winter, P., et al. (2003). Gene expression analysis of plant host-pathogen interactions by SuperSAGE. *Proceedings of the National Academy of Sciences*, 100(26), 15718-15723.
- Morris, J. S., Baggerly, K. A., & Coombes, K. R. (2003). Bayesian shrinkage estimation of the relative abundance of mRNA transcripts using SAGE. *Biometrics*, 59, 476-486.
- Stollberg, J., Urschitz, J., Urban, Z., & Boyd, C. D. (2000). A quantitative evaluation of SAGE. *Genome Research*, 10, 1241-1248.
- Thygesen, H. H., & Zwinderman, A. H. (2006). Modeling Sage data with a truncated gamma-Poisson model. *BMC Bioinformatics*, 7, 157.
- Velculescu, V. E., Zhang, L., Vogelstein, B., & Kinzler, K. W. (1995). Serial Analysis of Gene Expression. *Science*, 270(5235), 484-487.
- Velculescu, V. E., Zhang, L., Zhou, W., Vogelstein, J., Basrai, M. A., Bassett, J., D E, et al. (1997). Characterization of the yeast transcriptome. *Cell*, 88, 243-251.
- Vencio, R. Z. N., & Brentani, H. (2006). Statistical methods in serial analysis of gene expression(sage). In W. Zhang & I. Shmulevich (Eds.), *Computational and statistical approaches to genomics* (p. 209-233). New York: Springer Verlag. (2nd Edition)
- Wikipedia. (2007). *Poisson distribution*. ([Online; accessed 25-Oct 2007])

Tables

Table 1: Autocorrelation Estimates for the Dirichlet-Poisson-Binomial (DPB), Dirichlet-Multinomial-Binomial (DMB), and Missing Data algorithms.

Lag	DPB		MB		MD	
	N	N	N	N	r	N
	$(\alpha = 1)$	$(\alpha = 1/k)$	$(\alpha = 1)$	$(\alpha = 1/k)$	$(\alpha = 1)$	$(\alpha = 1/k)$
10	0.905	0.024	0.0001	-0.011	0.606	0.007
20	0.863	0.018	0.020	0.020	0.344	-0.012
40	0.783	-0.029	-0.027	-0.010	0.088	-0.034
80	0.666	0.027	-0.009	-0.018	-0.011	0.011

Table 2: Execution Times for Algorithms. 5 million samples collected. Number of genes $k = 6096$. Algorithms compared are Dirichlet-Poisson-Binomial (DPB) of Section 4.1, Dirichlet – Multinomial Binomial (DMB) of Section 4.2 and the Missing Data method (MD) described in Section 4.3.

Method	α	run time (min.)
DPB	1	750
DPB	1/k	730
DMB	1	30
DMB	1/k	50
MD	1	20
MD	1/k	19

Figure Captions

Figure 1. Plot showing cDNA cleavage sites for SAGE with associated probabilities of tag formation.

Figure 2. Probability estimates and inferences for the Dirichlet -Poisson -Binomial with each $\alpha_i = 1$. The 20 genes with the largest tag counts are arranged in decreasing rank order along the X-axis. The observed tag proportions are marked in dark circles, the standard MLE in dark triangles. The analytically computed posterior mode $\alpha_i = 1$ coincides exactly with the MLE. Also included are the estimated posterior mean and upper and lower 95% Bayesian Credible bounds based on MCMC sampling.

Figure 3. Probability estimates and inferences for the Dirichlet -Poisson -Binomial with each $\alpha_i = 1/k$. The 20 genes with the largest tag counts are arranged in decreasing rank order along the X-axis. The observed tag proportions are marked in dark circles, the standard MLE in dark triangles. In this case analytically derived posterior modes deviate substantially from MLE. However, estimated posterior mean is identical to MLE in this case. Upper and lower 95% Bayesian Credible bounds are also given.

Figure 4. Probability estimates for the Dirichlet -Multinomial -Binomial where all $\alpha_i = 1$. The 20 genes with the largest tag counts are arranged in decreasing rank order along the X-axis. The observed tag proportions are marked in dark circles, the standard MLE in dark triangles. The analytically computed posterior mode $\alpha_i = 1$ coincides exactly with the MLE. Also included are the estimated posterior mean and upper and lower 95% Bayesian Credible bounds based on MCMC sampling.

Figure 5. Probability estimates for the Dirichlet -Multinomial -Binomial model with all $\alpha_i = 1/k$. The 20 genes with the largest tag counts are arranged in decreasing rank order along the X-axis. The observed tag proportions are marked in dark circles, the standard MLE in dark triangles. In this case analytically derived posterior modes deviate substantially from MLE. However, estimated posterior mean is identical to MLE in this case. Upper and lower 95% Bayesian Credible bounds are also given.

Figure 6. Probability estimates for the Missing Data Algorithm where all $\alpha_i = 1$. The 20 genes with the largest tag counts are arranged in decreasing rank order along the X-axis. The observed tag proportions are marked in dark circles, the standard MLE in dark triangles. The analytically computed posterior mode $\alpha_i = 1$ coincides exactly with the MLE. Also included are the estimated posterior mean and upper and lower 95% Bayesian Credible bounds based on MCMC sampling.

Figure 7. Probability estimates for the Missing Data Algorithm where $\alpha_i = 1/k$. The 20 genes with the largest tag counts are arranged in decreasing rank order along the X-axis. The observed tag proportions are marked in dark circles, the standard MLE in dark triangles. In this case analytically derived posterior modes deviate substantially from MLE. However, estimated posterior mean is identical to MLE in this case. Upper and lower 95% Bayesian Credible bounds are also given.

Figures

Figure 1: Plot showing cDNA cleavage sites for SAGE with associated probabilities of tag formation.

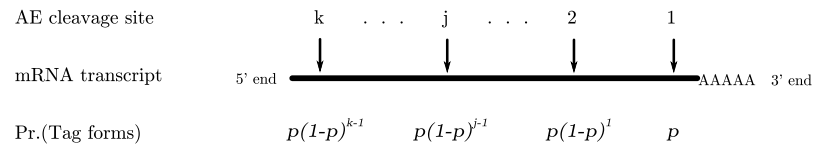


Figure 2: Probability estimates and inferences for the Dirichlet -Poisson -Binomial with each $\alpha_i = 1$. The 20 genes with the largest tag counts are arranged in decreasing rank order along the X-axis. The observed tag proportions are marked in dark circles, the standard MLE in dark triangles. The analytically computed posterior mode $\alpha_i = 1$ coincides exactly with the MLE. Also included are the estimated posterior mean and upper and lower 95% Bayesian Credible bounds based on MCMC sampling.

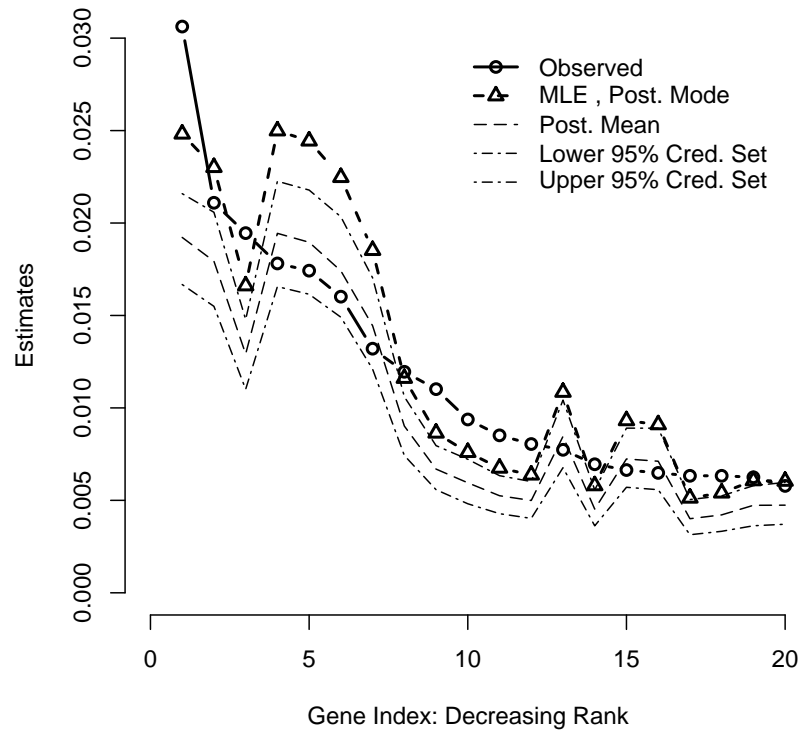


Figure 3: Probability estimates and inferences for the Dirichlet -Poisson -Binomial with each $\alpha_i = 1/k$. The 20 genes with the largest tag counts are arranged in decreasing rank order along the X-axis. The observed tag proportions are marked in dark circles, the standard MLE in dark triangles. In this case analytically derived posterior modes deviate substantially from MLE. However, estimated posterior mean is identical to MLE in this case. Upper and lower 95% Bayesian Credible bounds are also given.

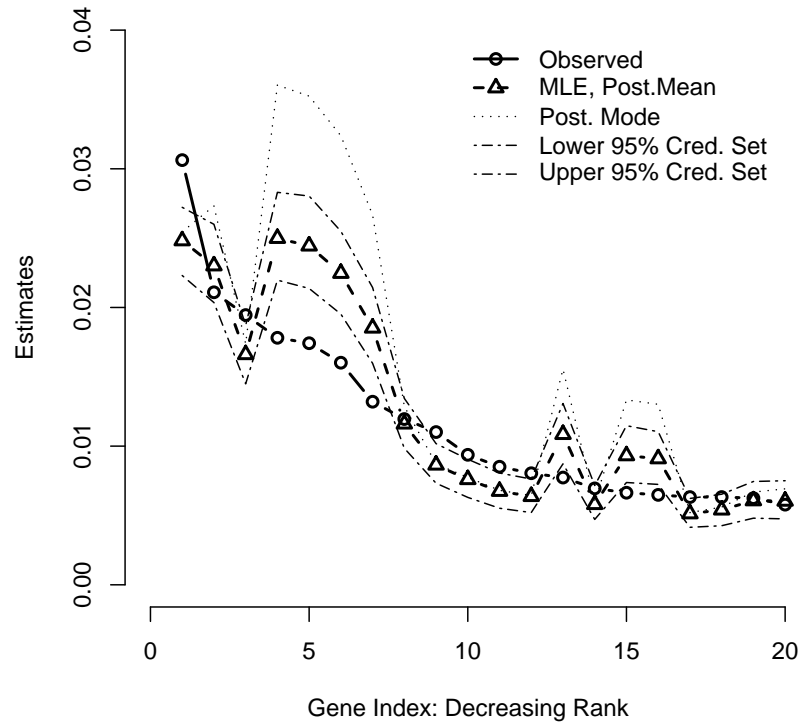


Figure 4: Probability estimates for the Dirichlet -Multinomial -Binomial where all $\alpha_i = 1$. The 20 genes with the largest tag counts are arranged in decreasing rank order along the X-axis. The observed tag proportions are marked in dark circles, the standard MLE in dark triangles. The analytically computed posterior mode $\alpha_i = 1$ coincides exactly with the MLE. Also included are the estimated posterior mean and upper and lower 95% Bayesian Credible bounds based on MCMC sampling.

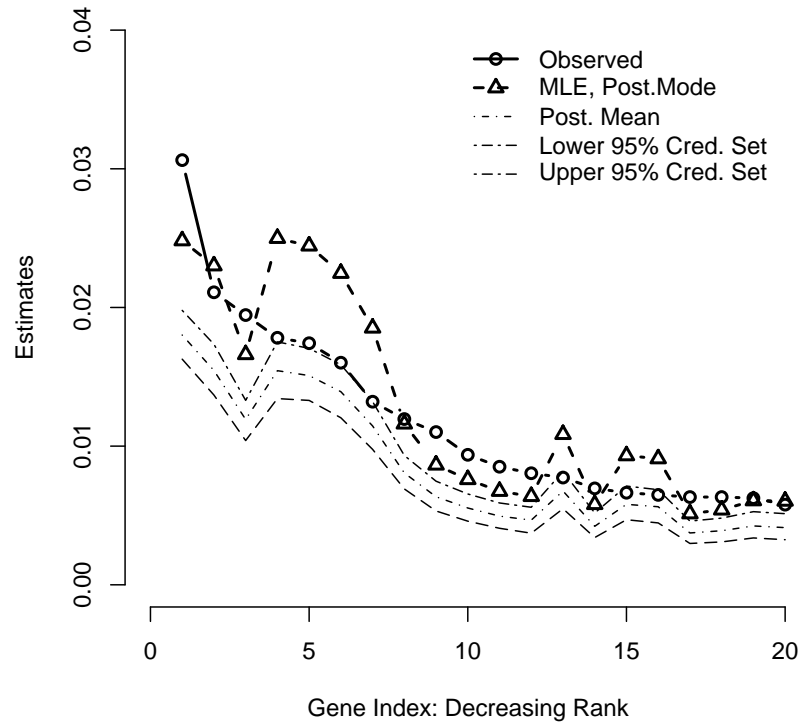


Figure 5: Probability estimates for the Dirichlet -Multinomial -Binomial model with all $\alpha_i = 1/k$. The 20 genes with the largest tag counts are arranged in decreasing rank order along the X-axis. The observed tag proportions are marked in dark circles, the standard MLE in dark triangles. In this case analytically derived posterior modes deviate substantially from MLE. However, estimated posterior mean is identical to MLE in this case. Upper and lower 95% Bayesian Credible bounds are also given.

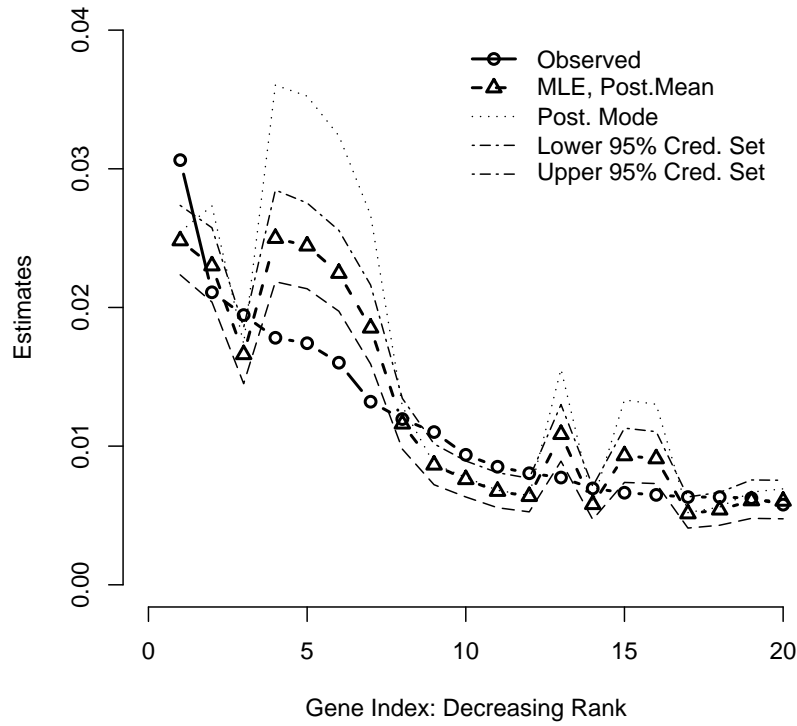


Figure 6: Probability estimates for the Missing Data Algorithm where all $\alpha_i = 1$. The 20 genes with the largest tag counts are arranged in decreasing rank order along the X-axis. The observed tag proportions are marked in dark circles, the standard MLE in dark triangles. The analytically computed posterior mode $\alpha_i = 1$ coincides exactly with the MLE. Also included are the estimated posterior mean and upper and lower 95% Bayesian Credible bounds based on MCMC sampling.

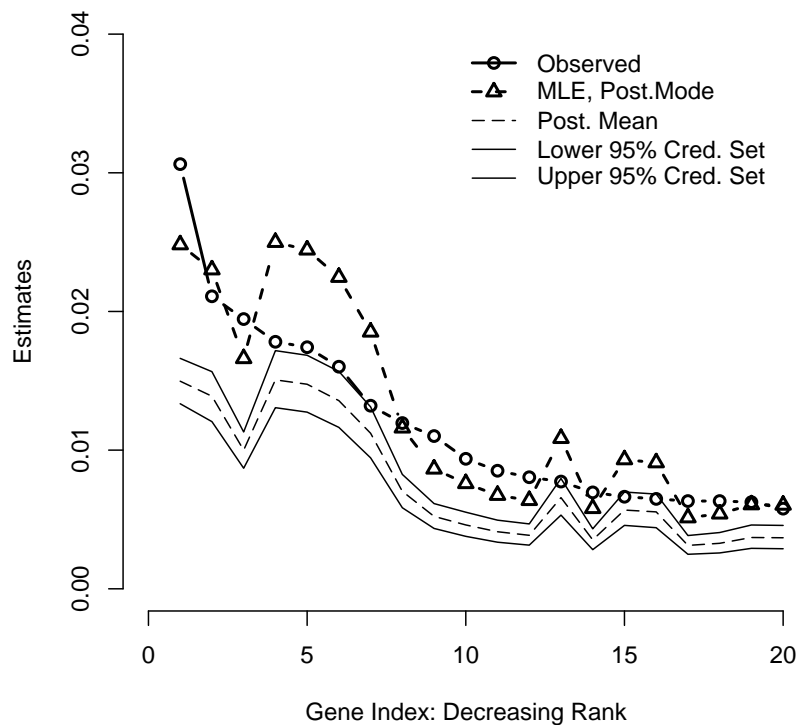


Figure 7: Probability estimates for the Missing Data Algorithm where $\alpha_i = 1/k$. The 20 genes with the largest tag counts are arranged in decreasing rank order along the X-axis. The observed tag proportions are marked in dark circles, the standard MLE in dark triangles. In this case analytically derived posterior modes deviate substantially from MLE. However, estimated posterior mean is identical to MLE in this case. Upper and lower 95% Bayesian Credible bounds are also given.

